# InGaAs CONCENTRATOR CELLS FOR LASER POWER CONVERTERS AND TANDEM CELLS[1]

S. Wojtczuk, S. Vernon and E. Gagnon
Spire Corporation, Bedford, MA 01730-2396

## Abstract

$In_{0.53}Ga_{0.47}As$ N-on-P concentrator cells were made as part of an effort to develop $1.315\mu m$ laser power converters. The $1.315\mu m$ laser power conversion efficiency was estimated as 29.4% (at 5.57 $W/cm^2$) based on an 86% measured external quantum efficiency at $1.315\mu m$, and a measured open circuit voltage (484mV), and fill-factor (67%) at the equivalent AM0 short-circuit photocurrent (5.07 $A/cm^2$). A 13.5% AM0 efficiency was achieved at 89 suns and 25C. Measured one-sun and 100-sun AM0 efficiency, log I-V analysis, and quantum efficiency are presented for InGaAs cells with and without InP windows to passivate the front surface. Windowed cells performed better at concentration than windowless cells. Lattice mismatch between InGaAs epilayers and InP substrate was <800 ppm. Theoretical efficiency is estimated for $1.315\mu m$ laser power converters versus the bandgap energy. Adding aluminum to InGaAs to form $In_xAl_yGa_{1-x-y}As$ is presented as a way to achieve an optimal bandgap for $1.315\mu m$ laser power conversion.

## Introduction

Solar cells are often used as power for space missions where sunlight is available. However, some applications (ref.1) such as satellites in eclipse, moon bases in lunar night, orbital transfer vehicles, and planetary rovers need power when sunlight is unavailable or require a higher power than the sun provides. Laser beams directed onto the solar cells can provide high power in these instances. In laser power conversion, the cell is optimized for the single laser wavelength and has a higher efficiency ($\approx$30-60%) than cells designed for sunlight ($\approx$15-25%), where compromises are made in design in order to extract the most power from the multiple-wavelength solar spectrum. Achieving the best overall power conversion efficiency involves optimizing both source (laser) and receiver (solar cell) power efficiency. We present data on solar cells useful for converting $1.315\mu m$ laser radiation. This wavelength is of interest because of the existence of high-efficiency $1.315\mu m$ iodine lasers and power conversion systems explored by Walker et al. (ref.2).

Indium gallium arsenide ($In_{0.53}Ga_{0.47}As$) single-junction N-on-P cells used as laser power converters (LPCs) are investigated. The $In_{0.53}Ga_{0.47}As$ ("InGaAs" henceforth) is lattice-matched to indium phosphide (InP) substrates. Measured AM0 and quantum efficiency data are used to estimate the laser power converter (LPC) efficiency at $1.315\mu m$ (29.4%). The 0.75eV bandgap of InGaAs is slightly sub-optimal for $1.315\mu m$ laser power conversion. Adding aluminum to InGaAs to form $In_xAl_yGa_{1-x-y}As$ is suggested to increase the bandgap towards the optimal 0.9eV energy, while maintaining InP lattice match. Theoretical efficiency limits for $1.315\mu m$ LPCs versus the bandgap are presented. These single-junction LPCs can use laser powers of $\approx$5 $W/cm^2$ (about 100 AM0 suns). For higher power (e.g.100 $W/cm^2$), a single junction LPC has excessive $I^2R$ loss. Spire plans to eventually series-connect (boosting voltage) many small junctions over the same area as the larger single junction, to lower photocurrent and $I^2R$ loss, similar to how a generating station transmits power to consumers at high-voltage to avoid $I^2R$ loss through miles of copper. Multijunction LPCs have been implemented in GaAs technology (ref. 3,4). Finally, the cells and data reported are also of interest as bottom cells of high efficiency InP/InGaAs two-junction tandems (ref. 5,6).

---

## Laser Power Converter Material Growth and Device Fabrication

The InGaAs layers (Table I) used were grown in a Spire 100S single-wafer metal organic chemical vapor deposition (MOCVD) epitaxial reactor under conditions summarized in Table II on $P^+$ InP substrates. Two structures were used, one with the window and cap, and the other omitting those two layers.

Table I  InGaAs LPC Epilayer Structures.

| Thickness (μm) | Doping Type | Doping (cm$^{-3}$) | Material | Purpose |
|---|---|---|---|---|
| 0.3 | N | $10^{19}$ | InGaAs | Contact Cap |
| 0.5 | N | $10^{18}$ | InP | Window |
| 0.3 | N | $10^{18}$ | InGaAs | Emitter |
| 2.7 | P | $10^{17}$ | InGaAs | Base |
| 0.3 | P | $10^{19}$ | InP | Back Surface Field |
| 300 | P | $10^{18}$ | InP | Substrate |

Table II  InGaAs Growth Parameters in a Spire 100S MOCVD Reactor.

| | |
|---|---|
| Growth Pressure | 76 torr |
| Growth Temperature | 600 °C |
| Wafer Rotation | 15 rpm |
| Hydrogen Mainflow | 2 slpm |
| Indium Source, Bubbler Temperature | Ethyldimethylindium, +10° C |
| Gallium Source, Bubbler Temperature | Trimethylgallium, -10° C |
| Arsenic Source | 100% Arsine |
| V to III Ratio | ≈400:1 |
| Growth Rate | ≈7Å/s or 2.5μm/hr |
| P-type Dopant | Dimethylzinc, 1000ppm diluted in $H_2$ |
| N-type Dopant | Silane, 500ppm diluted in $H_2$ |

The $N^+$ InGaAs contact cap allows a lower resistance ohmic contact to be made to the low bandgap InGaAs (0.75eV) than could be made to the high bandgap InP (1.34eV) window. The cap is later etched off everywhere but underneath the front metal contacts, since InGaAs absorbs 1.3μm light strongly, and carriers generated in the cap cannot diffuse through the InP window and are lost to recombination. The $N^+$ InP window lowers the recombination velocity at the $N^+$ InGaAs emitter front surface, and should decrease dark current and increase quantum efficiency at 1.3μm. The thick 0.5μm InP window is not best for AM0 power conversion, since the visible sunlight with energy above the InP bandgap is absorbed. However, the thick InP window lowers series resistance without appreciably absorbing 1.3μm light, an important design point for these high current 1.315μm converters. The absorption length of $In_{0.53}Ga_{0.47}As$ at 1.3μm is ≈0.8μm, so the 3μm InGaAs emitter and base regions absorb ≈98% of 1.3μm light.

Figure 1 is an outline of the fabrication process for cells with windows. Cells without windows are made using a similar, simpler process. Figure 2 shows a picture of a completed cell.
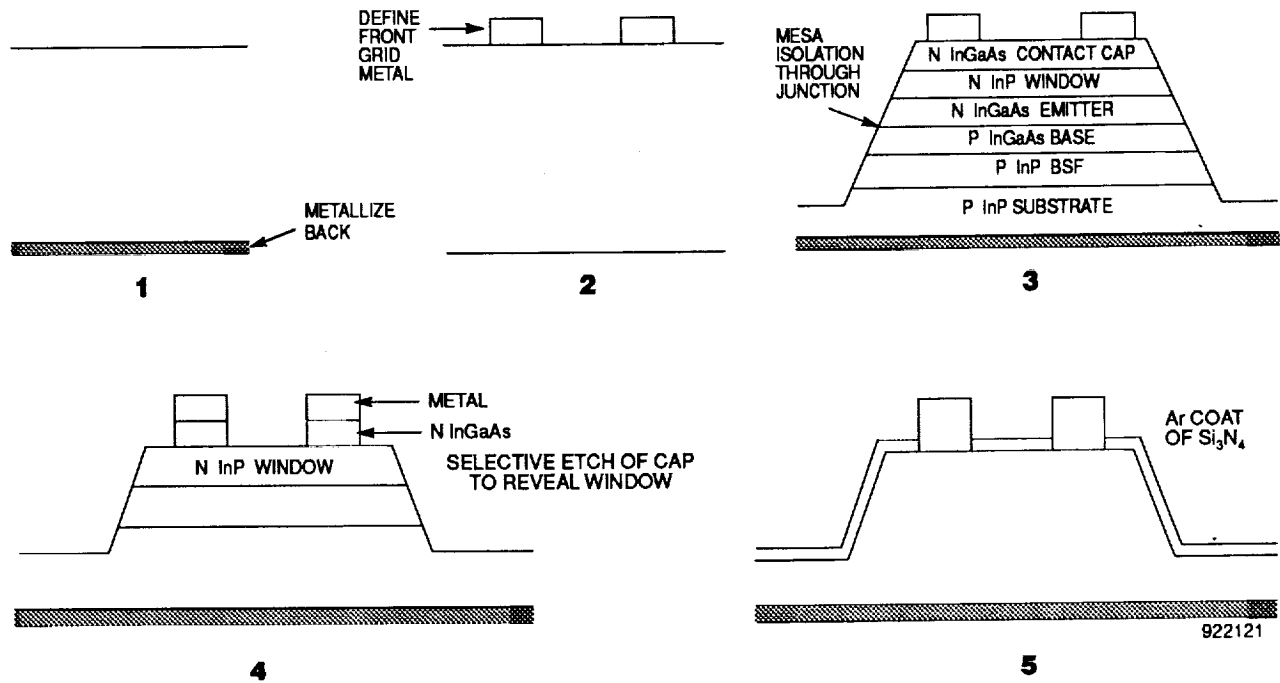


Figure 1    Simplified converter fabrication process. 1) Metallize backs. 2) Define front contact grid. 3) Isolate devices. 4) Strip InGaAs contact cap from photoarea. 5) Anti-reflection coating.
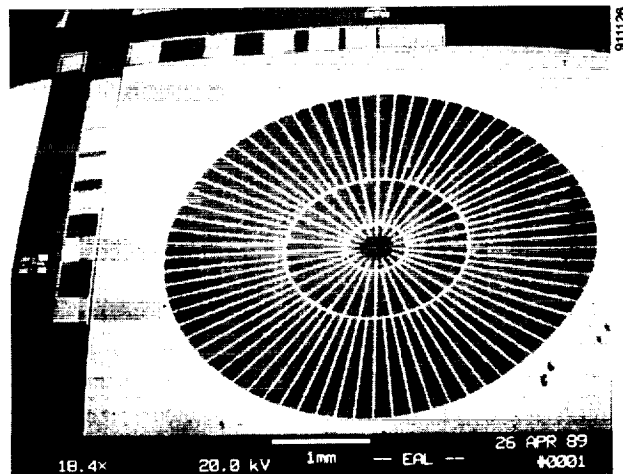


Figure 2    Scanning electron micrograph of an LPC. Photoarea is 0.136 cm$^2$, ≈4mm in diameter. P-N junction area is 5mm square (0.25 cm$^2$). Grid lines are 3μm wide and 3μm high.

121

The process used is briefly described below:

1) (BACK METALLIZATION) Protect epilayers with $Si_3N_4$. Clean InP wafer backs by HCL etching. Metallize backs of the $P^+$ InP wafers with thermally evaporated AuZn and vacuum anneal.

2) (FRONT METALLIZATION) Photolithographically define front contact grids in photoresist using image reversal process, clean surface with $NH_4OH:H_2O$, plasma etch in $O_2$ to remove any resist residue, clean oxides in openings with a buffered HF dip, electron-beam evaporate Cr/Ag/Au front grid metal. Liftoff excess metal with an acetone soak, leaving the front contact grid metal.

3) (DEVICE ISOLATION) Photolithographically cover device area with photoresist. Selectively etch off 0.3μm InGaAs cap from exposed areas with $1H_3PO_4:1H_2O_2:8H_2O$. Selectively etch 0.5μm InP window off in HCL. Selectively etch InGaAs layers using 1:1:8 etch. Dektak wafers to determine actual thickness of etched material to insure junctions are isolated between devices.

4) (CAP STRIP FROM PHOTOACTIVE AREA) Selectively etch off the 1.3μm light-absorbing InGaAs contact cap from the active device area with the 1:1:8 etch, using the front-grid metal as a self-aligned mask. No photolithography needed.

5) (ANTI-REFLECTION COATING) Plasma deposit $Si_3N_4$ for a quarter wave AR coat optimized at 1.3μm. Final photolithography step removes silicon nitride off the front contact busbar.

## $In_{0.53}Ga_{0.47}As$ Laser Power Converter Cell Test Data

The 1.315μm laser power conversion efficiency was estimated at 29.4% (at 5.57 $W/cm^2$). We assumed an incident 1.315μm laser power density of 5.57 $W/cm^2$ because the measured external quantum efficiency of 86% at 1.315μm gives a short-circuit photocurrent of 5.07 $A/cm^2$ with 5.57 $W/cm^2$ of 1.315μm laser power. Measured AM0 concentration data at this same current density (Table III) should accurately give the open-circuit voltage (484mV) and fill-factor (66.8%) the cell would exhibit if operated as a converter under this laser illumination. These values were used to estimate the efficiency, as described later. Table III summarizes AM0 efficiencies, open-circuit voltages ($V_{oc}$), short circuit currents ($I_{sc}$), short-circuit current densities ($J_{sc}$), and fill-factors (FF) measured at Spire. Cells were made on 2-inch InP $P^+$ wafers; there were 29 cells on each wafer as well as several diagnostic test patterns. Both one-sun data for the best cell and average data for all 29 cells is reported. This AM0 data is useful in evaluating the performance of these devices as bottom cells of InP/InGaAs high efficiency two-junction tandems cells. Also, as explained above, the AM0 concentration tests allow measurements of $V_{oc}$, FF, and series resistance effects at the high photocurrents which would occur under laser testing. The antireflection coating and InP windows were optimized for 1.315μm and not for the broad AM0 spectrum.

The InGaAs cells with InP windows had higher AM0 efficiencies at concentration, since they had better quantum efficiency, and because the thick InP window lowers the emitter sheet series resistance (higher FF). In contrast, windowless cells had their FF drop at concentration, implying a series resistance problem in the thin emitter at high currents. Photocurrents of windowless cells were less than windowed cells, which was somewhat surprising since the InP window absorbs visible AM0 light. Presumably, high surface recombination at the exposed InGaAs emitter surface lowered the minority lifetimes in the emitter more than we expected, reducing the photocurrent. This surface is passivated when the InP window is added, which is the probable reason why the cells with windows had higher photocurrents, although there could be some photocurrent collection from the InP window itself. InGaAs cells without windows had slightly better one-sun efficiencies, despite the lower photocurrent, because of higher photovoltages at one-sun, which is probably due to their lower dark current in the one-sun bias region. The lower generation-recombination space charge current of the windowless cells may be due to the excellent lattice matching (<280ppm) achieved in this cell run.

## Table III  Spire AM0 Efficiency Tests.

| Converter ID | Voc V | Isc mA | Jsc mA/cm² | AM0 Suns | Fill % | Eff % | Comments |
|---|---|---|---|---|---|---|---|
| InGaAs n/p Cell with InP Window - lattice mismatch 790ppm | | | | | | | |
| 5501-1425-21 | 0.287 | 7.781 | 57.21 | 1 | 57.1 | 6.83 | Best cell |
| 5501-1425-21 | 0.484 | 690.2 | 5074.80 | 88.7 | 66.8 | 13.5 | Best cell |
| average | 0.279 | 7.773 | 57.16 | 1 | 56.6 | 6.58 | Average of all 29 cells |
| average | 0.483 | 701.6 | 5158.73 | 90 | 65.3 | 13.2 | Average of 6 cells |
| InGaAs n/p Cell with No Window - lattice mismatch 280ppm | | | | | | | |
| 5501-1419-18 | 0.305 | 6.174 | 45.40 | 1 | 70.8 | 7.14 | Best cell |
| 5501-1419-18 | 0.439 | 656.2 | 4825.0 | 106 | 65.8 | 9.57 | Best cell |
| average | 0.298 | 6.078 | 44.69 | 1 | 67.4 | 6.57 | Average of 29 cells |
| average | 0.436 | 620.7 | 4564.06 | 102 | 62.4 | 8.91 | Average of 6 cells |

The measured external quantum efficiency and reflectance is shown in Figure 3 for a typical InGaAs converter with and without InP windows.
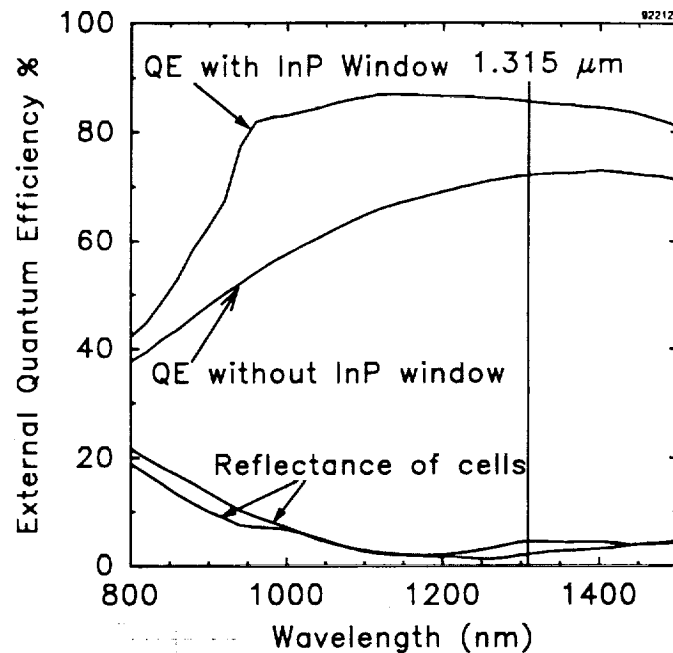


Figure 3    External quantum efficiency and reflectance measured for InGaAs LPCs.

InGaAs has a cutoff wavelength of 1.65μm, which is off the plot in Figure 3. The quantum efficiency roll-off in the InGaAs LPCs without InP windows below 1200nm is probably due to the high surface recombination at the unpassivated InGaAs emitter front surface. For the InGaAs LPCs with an InP window, the quantum efficiency is strikingly improved above 900nm, due to the InP window (minority carrier mirror) separating the photogenerated carriers in the InGaAs from the surface. Below 920nm, the InP window is itself absorbing, and the photogenerated carriers created in the InP window due to this light are again lost to surface recombination. The InP/InGaAs interface recombination is clearly low enough so that we gain an appreciable advantage in quantum efficiency using windowed structures.

Converter I-V data are shown in Figure 4. Windowless InGaAs junctions had lower lattice mismatch (280ppm, measured by X-ray diffraction) and lower dark current. The windowless junctions are diffusion current limited; the cells with windows are dominated by space-charge recombination current. Table IV shows the I-V least-squares fit to a simple diode model to extract the relative contributions of the diffusion current versus the space-charge region recombination current.
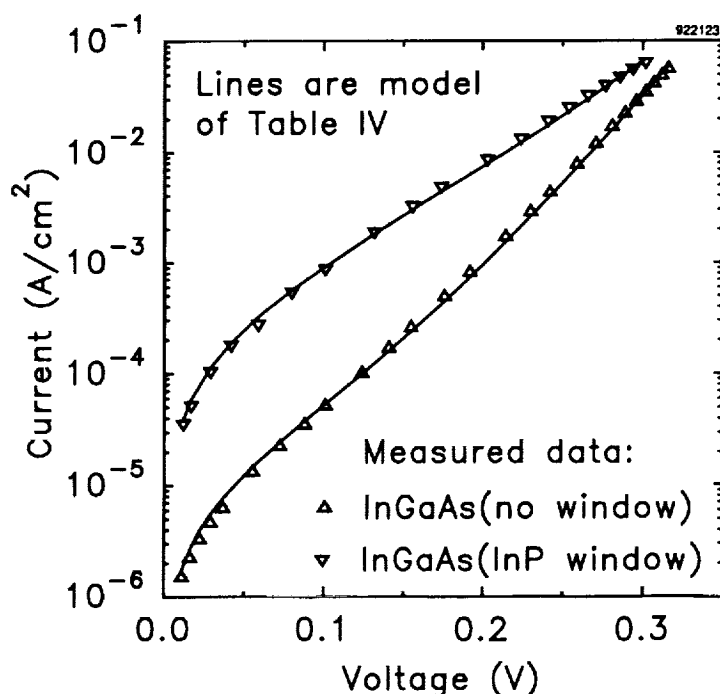


Figure 4        Log I-V curves of InGaAs junction with (ID#1419) and without (ID# 1425) InP window.

Table IV        Diffusion and Space Charge Recombination Current Components Fit to Measured InGaAs LPC IVs.

| ID # | Diffusion Current Jo1 (A/cm$^2$) | Space-charge Current Jo2 (A/cm$^2$) | Comments |
|---|---|---|---|
| 1419-24 | $2.7 \times 10^{-7}$ | $6.6 \times 10^{-6}$ | no window, 280 ppm mismatch |
| 1425-14 | $1.4 \times 10^{-7}$ | $1.5 \times 10^{-4}$ | InP window, 790 ppm mismatch |
| $J = Jo1 [ \exp (qV/kT - 1)] + Jo2 [ \exp (qV/2kT - 1)]$ | | | |

## Theoretical Laser Power Converter Efficiency versus Bandgap

In this section, laser power converter efficiency versus semiconductor bandgap is modeled, with the goal of estimating the increase in 1.315μm converter efficiency if a bandgap higher than $In_{0.53}Ga_{0.47}As$ (0.75eV) is used. The short-circuit photocurrent $J_{SC}$ (units: A/cm$^2$) for monochromatic light is:

$$J_{SC} = \frac{q(QE)P\lambda}{hc} \quad or \quad \frac{J_{SC}}{P} = 1.06 \, QE \quad (A/W \, at \, 1.315 \, \mu m) \tag{1}$$

Here "q" is the electron charge (C), "QE" the external quantum efficiency at the laser wavelength "λ" (m), "P" the incident laser power (W/cm$^2$), "h" Planck's constant (J-s), and "c" the velocity of light (m/s). $J_{SC}$ is to first-order independent of bandgap since "QE" is to first order also independent of bandgap. The dark current limit $J_0$ (A/cm$^2$) versus direct bandgap energy can be estimated simply as (ref.7):

$$J_O = \frac{2\pi kTq^3(n^2+1)E_G^2}{10,000 h^3 c^2} \exp\left(-\frac{qE_G}{kT}\right) \approx 6,960 \, E_G^2 \exp\left(-\frac{E_G}{0.026}\right) \tag{2}$$

This is "perfect" dark current assuming radiative-limited lifetimes and no surface recombination, derived from detailed balance equations for photon absorption and radiative recombination. As a check, the formula predicts about half the diffusion current of very good GaAs cells. "k" is Boltzmann's constant (J/K), "T" is the temperature (K), "n" is the refractive index at the laser wavelength, and "$E_G$" is the bandgap voltage (V). The above approximation uses an "n" of 4 and a 300K "T". The open-circuit voltage $V_{OC}$ is then:

$$V_{OC} = \frac{kT}{q} \ln\left(\frac{J_{SC}}{J_O} + 1\right) \tag{3}$$

The fill-factor (FF) was calculated numerically for the theoretical data presented below. However, for a single-junction cell with no series resistance, excellent agreement (to three places) exists between the numerical calculations for the fill-factor and an analytical formula by Green (ref.8):

$$FF = \frac{v - \ln(v + 0.72)}{v + 1} \tag{4}$$

"$v$" is the normalized voltage variable (q$V_{OC}$/kT). The laser power conversion efficiency η is then:

$$\eta = \frac{V_{OC} \, J_{SC} \, FF}{P} \tag{5}$$

125

Using the above formulae, upper theoretical efficiency limits for 1.315μm laser power converters as a function of bandgap are shown in Figure 5, ranging from the 0.75eV bandgap energy of $In_{0.53}Ga_{0.47}As$ to near the 0.94eV photon energy of the 1.315μm wavelength laser light. The assumptions are:

1) 100% external quantum efficiency at 1.315μm
2) "perfect" radiative-lifetime-limited dark current as in the approximate equality of equation (2)
3) room temperature operation
4) no series resistance
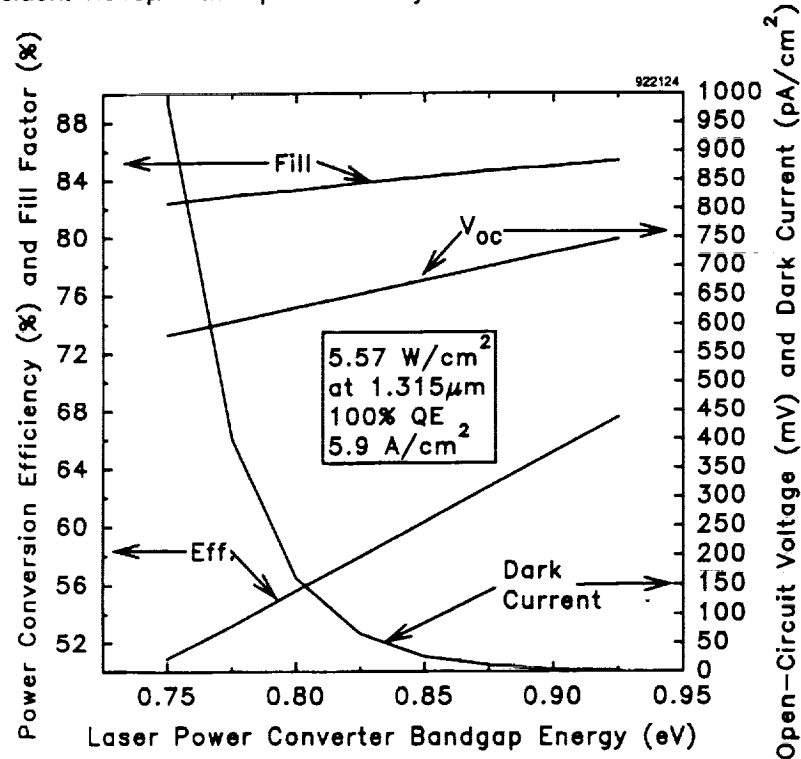5) 5 W/cm² incident 1.315μm laser power density



Figure 5    Upper theoretical efficiency limits for a 1.315μm laser power converter as a function of the semiconductor bandgap of the converter material.

Table V compares theoretical predictions versus measured data achieved in this work. Of the parameters, we believe it is relatively easy to improve $J_{sc}$ (i.e. approach 100% external quantum efficiency at the single 1.315μm wavelength), and to reduce the series resistance further to improve FF somewhat. However, to improve $V_{oc}$ and FF toward their theoretical limits, dark currents will have to be reduced substantially by lowering surface/interface recombination velocities and space-charge dark currents, and increasing material lifetime toward the radiative limit , a very challenging task.

Table V    Upper Theoretical Limits versus Achieved Data for 0.75eV InGaAs 1.315μm Converters.

|  | $V_{oc}$ (mV) | $J_{sc}$ ( A/cm²) | FF (%) | Eff. (%) |
|---|---|---|---|---|
| Theory (Figure V) | 582 | 5.9 | 82 | 50 |
| Achieved (Table III) | 484 | 5.1 | 67 | 29 |
| Theoretical/Achieved | 83% | 86% | 82% | 58% |

InGaAs converters are not optimum for 1.315µm laser power conversion due to the 190meV energy difference between the 0.75eV bandgap and 0.94eV photon energies, which is wasted as heat. This lost power can be recovered if a higher bandgap converter is used, as Figure 5 illustrates. Lower indium composition $In_xGa_{1-x}As$ ( X < 0.53 ) has a higher bandgap, but the grown film is no longer lattice matched to the InP wafer, which generates stress-relieving dislocations in the material that act as recombination centers, decreasing minority carrier lifetimes and lowering efficiency. However, some compositions of $In_xAl_yGa_{1-x-y}As$ (Figure 6) can be grown with bandgaps approaching the 0.9eV optimum, while maintaining lattice match to InP. InAlGaAs is of great interest since it may be easier to grow by MOCVD than InGaAsP, which covers about the same bandgap and wavelength range. InAlGaAs is a III-III-III-V quaternary material, with only one group V element. It is relatively easy to grow, since the material composition is adjusted by controlling the gas flows of similar group III's, which incorporate into the material similarly. In contrast, InGaAsP, a III-III-V-V quaternary, needs to control not only the group III ratio, but the group V ratio as well. The arsine and phosphine gases used to supply the group V's work best at quite different material growth temperatures, making InGaAsP growth inherently more difficult.
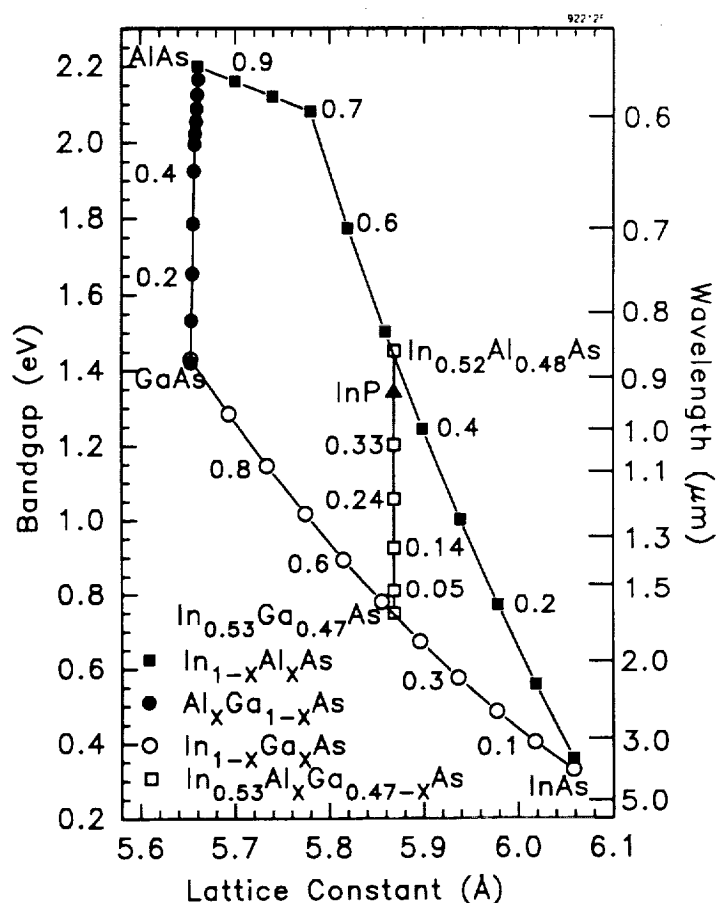


Figure 6    Bandgap vs. lattice-constant for $In_xAl_yGa_{1-x-y}As$ quaternary. Vertical line is the composition of $In_xAl_yGa_{1-x-y}As$ lattice matched to InP. Raw data from Madelung (ref.9).

## Conclusions

In this work, we describe the epitaxial growth, fabrication, and test results of single-junction 0.75eV $In_{0.53}Ga_{0.47}As$ laser power converters. Although we lacked a high power laser to do direct measurements, we estimate the 1.315$\mu$m laser power conversion efficiency as 29.4% (at 5.57 W/cm$^2$) based on an 86% measured external quantum efficiency at 1.315$\mu$m, and a measured open circuit voltage (484mV), and fill-factor (67%) at the equivalent AM0 short-circuit photocurrent (5.07 A/cm$^2$). Absolute external quantum efficiency and reflectance, IV data, and AM0 one-sun and concentration efficiencies were measured for InGaAs cells without and with InP windows to passivate the front surface of the emitter layer. Cells with InP windows had the highest external quantum efficiency (86% at 1.315$\mu$m), as well as the highest AM0 efficiencies under concentration (13.5%, 89 suns). Theoretical efficiency estimates were made for 1.315$\mu$m laser power converters versus the cell bandgap energy. Adding aluminum to InGaAs to form $In_xAl_yGa_{1-x-y}As$ is presented as a way to achieve an optimal bandgap for 1.315$\mu$m laser power conversion, and efficiencies over 60%.

## References

1.    Landis, G.A.: "Photovoltaic Receivers for Laser Beamed Power in Space," Proc. of 22nd IEEE PVSC, pp.1494-1502, (1991).

2.    Walker, G.H. and Heinbockel, J.H.: "Mathematical Modeling of a Photovoltaic-Laser Energy Converter for Iodine Laser Radiation," NASA Tech. Memo. 100482, (1987).

3.    Borden, P.G.: "A Monolithic Series-Connected AlGaAs/GaAs Solar Cell Array", Proc. of 14th IEEE PVSC, pp.554-562., (1980).

4.    Spitzer, M.B.; McClelland, R.W.; Dingle, B.D.; Dingle, J.E.; Hill, D.S.; and Rose, B.H.: "Monolithic Series-Connected Gallium Arsenide Converter Development", Proc. of 22nd IEEE PVSC, pp.142-146, (1991).

5.    Osterwald, C.R.; Wanlass, M.W.; Ward, J.S.; Keyes, B.M.; Emery, K.A.; and Coutts, T.J.: "Modeled Performance of Monolithic, 3-Terminal InP/InGaAs Concentrator Solar Cells as a Function of Temperature and Concentration Ratio", Proc. of 22nd IEEE PVSC, pp.216-219, (1991).

6.    M.W. Wanlass, T.J. Coutts, J.S. Ward, K.A. Emery, T.A. Gessert, and C.R. Osterwald, "Advanced High-Efficiency Concentrator Tandem Solar Cells", Proc. of 22nd IEEE PVSC, pp. 38-45, (1991).

7.    Henry, C.H.: "Limiting efficiencies of ideal single and multiple energy gap terrestrial solar cells", J. Appl. Phys. 51(8), pp.4494-4500., (1980).

8.    Green, M.A.: "Solar Cells", Prentice-Hall, p.80, (1982).

9.    Madelung, O. (Ed.): "Semiconductors - Group IV Elements and III-V Compounds", Springer-Verlag, (1991).